

## Performance Analysis of SUnSAL

Khushbu K. Matiada  
Sarvajanik College of Engineering &  
Technology Surat, India.  
khushbuec49@gmail.com

Prof. Naresh Patel  
Sarvajanik College of Engineering &  
Technology Surat, India.  
khushbuec49@gmail.com

**Abstract**— In Remote Sensing (RS) cameras, used for earth observation, are generally mounted on satellite or on aero plane. Due to very high altitude of Hyperspectral Cameras (HSCs) the spatial resolution of images taken by such camera is very poor, in order of 4 m by 4m to 20m by 20m. So a single pixel from image taken by HSC may contain more than one materials and it is not possible to know about the materials present in single pixel. HSC measures the reflectance of object in the wavelength of range from 0.4 to 2.5um at 200 bands with spectral resolution of 10nm. High spectral resolution enables the accurate estimation of number of materials present in scene, known as endmembers, their spectral signature and fractional proportion within pixel, known as abundance map. This process is known as Hyperspectral Unmixing (HU). Due to large data size, environmental noise, endmember variability, not availability of pure endmembers HU is a challenging task. HU enables various application like an agricultural assessment, environmental monitoring, change detection, mineral exploitation, ground cover classification, target detection and surveillance. There are three approaches to solve this task: Geometrical, statistical and sparse regression. First two methods are Blind Source Separation (BSS) techniques. Third approach is based on sparsity and considered as semi-blind approach because it assumes the availability of spectral library. Spectral library contains the spectral signatures of various materials measured on the earth surface using advance Spectro radiometers. In sparse unmixing a mixed pixel is represented in the form of linear combination of a number of spectral signature known in advance and available in standard library. In this paper, mathematical steps for Spectral Unmixing using variable Splitting and Augmented Lagrangian (SUnSAL) are simplified. performance of SUnSAL is evaluated with the help of standard and publically available synthetic data base.

**Keywords**- *Imaging, Spectral Unmixing, Spectral Signature, Sparse Regression, ADMM, SUnSAL.*

\*\*\*\*\*

### I. INTRODUCTION

Remote Sensing (RS) is the field of science for obtaining information about objects or area, without any physical contact with it, from satellite or aircraft. Remote sensors placed on satellite or can be on aircraft. Remote sensors collect data by processing energy that is reflected from earth surface. The term “Remote Sensing” was first introduced in 1960 by Evelyn L. Pruitt of the U.S. office of Naval research. Hyperspectral Cameras (HSC) contribute significantly to earth observation and remote sensing. HSCs are built to work in many regions of the electromagnetic spectrum. The HSCs can be operate in the visible, near-infrared and shortwave infrared spectral bands of range 0.4 to 2.5um [1]. Spectral imaging widely used in remote sensing because of its broad applications in agricultural and environmental monitoring, mineral exploration, military surveillance and so on [2]. Due to low spatial resolution of HSCs, multiple scattering, microscopic material mixing and spectral measured by HSCs are mixtures of spectral signature of materials in a scene. However, due to low spatial resolution of imaging sensor, a single pixel is often composed of more than one different materials, leading to mixed pixel problem [2]. So, unmixing is required for accurate estimation. Pixels are mixtures of a few materials which is called endmembers [1]. Unmixing involves estimation of the number of endmembers, their spectral signatures and their abundances at each pixel [1]. Unmixing is a challenging task, ill-posed inverse problem because of large data size, model inaccuracies, observation noise, different environmental conditions and endmember variability [1]. Multispectral image

has some limitations: Low spectral Resolution and Low spatial Resolution. This Limitations of Multispectral image are overcome by Hyperspectral image. Hyperspectral image captures more narrow bands than multispectral image in the same portion of the EMS (Electro Magnetic Spectrum). The accurate estimation of number of materials present in scene, which is known as Endmembers. Their spectral signature and fractional proportion within pixel, known as Abundance map. This process is known as Hyperspectral Unmixing. For spectral unmixing, a Linear Mixture Model (LMM) is often used to capture the mixing behaviour of mixed pixels [2]. This model assumes that the observed spectrum of a pixel is a linear combination of a collection of endmembers weighted by the corresponding abundances [2]. Based on LMM, spectral unmixing consists of two procedures: (1) endmember extraction (2) abundance recovery [2]. Endmember extraction is to find and identify the endmembers presented in the scene. Abundance recovery is a linear inverse problem that is one of the most important mathematical problems [2].

Hyperspectral images are 3-dimensional arrays with two spatial dimensions and one spectral dimension. There are 3 basic approach of HU. First is Geometrical based approach, second is Statistical based and third is Sparse regression based approach. First two approaches are Blind and third one is Semi Blind approach. In first approach there is only observed image and no other data, from observed image we have to estimate signature of endmember and abundance of matrix. In rest of two, observed image and partial information of spectral signature, so it is known as semi blind approach. High level of

sparsity is useful to mitigate highly correlated spectral signatures.

Sparse unmixing has been introduced in HIS to characterize mixed pixels. It assumes that the observed image signatures can be expressed in the form of linear combinations of a number of pure spectral signatures known in advance. The sparsity prior, which assumes that few elements of the signals in the original domain are nonzero, has received extensive attentions in many applications [2]. There are some standard libraries which is publically available like USGS (U.S. Geological Survey), which has more than 1300 spectral signatures and ASTER (Advanced Spaceborne Thermal Emission and Reflection Radiometer) Spectral library, which contain over 2400 spectral signatures. These libraries used to guarantee accuracy in practical applications because of several reasons. When, distinct materials are combined into a microscopic (intimate) mixture [13]. Section 2 describes the Linear Mixing Model. Section 3 describes the sparse unmixing approach for Hyperspectral images. Section 4 shows the MATLAB simulation for synthetic data using SUNSUL algorithm. Conclusion and future work presents in section 5.

## II. MIXING MODEL

As per linear mixing model (LMM) the observed spectral signature of a mixed pixel is assumed to be linear combination of spectral signatures of endmembers present in respective pixel as shown in figure 1 [1]. For each single pixel of 3-dimensional hyperspectral data cube the LMM can be written as,

$$y_i = \sum_{j=1}^q A_{ij}x_j + n_i \quad (1)$$

Where the subscript  $i$  represents the spectral band number and subscript  $j$  represents the endmember number from endmember matrix. The length of observed vector  $y$  is  $L$ , i.e.  $i=1, 2, \dots, L$ . and number of endmembers in endmember matrix are  $q$ , i.e.  $j=1, 2, \dots, q$ .  $A_{ij}$  represents the reflectance at spectral band  $i$  of  $j$ th endmember. The fractional proportion of  $j$ th endmember in a pixel is given by  $x_j$ .  $n_i$  represents the error term for the spectral  $b$  and  $i$ . In general, mathematically LMM can be written in compact form as

$$y = Ax + n \quad (2)$$

Where  $y \in R^L$  is a observed spectral vector,  $A \in R^{L \times q}$  is endmember matrix containing  $q$  pure spectral signatures  $x \in R^q$  is fractional abundances of the endmembers for a given pixel, and  $n \in R^L$  is the errors which affecting the measurements at the each spectral band [13].

The value of fractional abundance is always nonnegative, lie in the range of 0 to 1 and sum of its values for single pixel is always one. These are known as Abundance non-Negativity Constraint (ANC) Abundance Sum-to-one

Constraint (ASC), which are represented in compact form as  $x_j \geq 0$  and  $\sum_{j=1}^q x_j = 1$  [3].

In the problem of LSU, given a hyperspectral data cube  $Y$  and the objective is to estimate the endmembers signatures and their fractional abundances, denoted by  $M$  and  $x$  for each pixel of the image respectively.

## III. SPARSE UNMIXING: SIMPLIFIED APPROACH

The priori availability of spectral libraries has increased interest in sparse unmixing. Sparse unmixing has two important drawbacks like the difficulty of estimating the number of endmembers and the process of extracting the endmembers itself, the result of which will vary according to the utilized extraction method [1]. The mixed pixel can be expressed in the form of linear combination of a number of spectral signature known in advance and it is available in standard library [13]. There are some standard libraries which is publically available like USGS (U.S. Geological Survey), which has more than 1300 spectral signatures and ASTER (Advanced Spaceborne Thermal Emission and Reflection Radiometer) Spectral library, which contain over 2400 spectral signatures. The use of image-derived endmembers may not result in accurate fractional abundance estimations, it can be like that such endmembers may not be completely pure in nature [13].

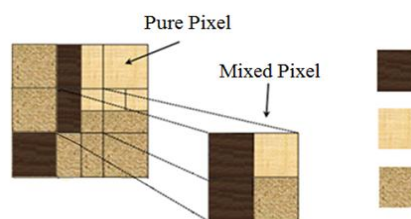


Figure (a)

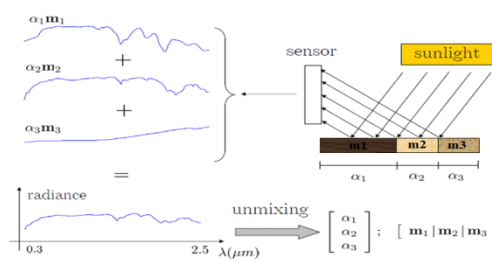


Figure (b)

Figure 1 (a)Concept of Mixed Pixel (b) Linear Mixing scenario for a single pixel in HIS.

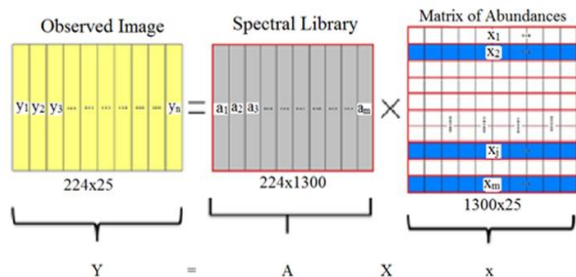


Figure 2. Sparse Regression Based Approach [2].

The mixtures is obtained at the particle level, the use of image-derived spectral endmembers cannot accurately characterize the different spectral mixtures. When, distinct materials are combined into a microscopic mixture.

A sparse signal is exactly recoverable from an underdetermined linear system of equations in computationally efficient manner. Let  $A \in R^{l \times m}$ ,  $l < m$ , where  $l$  is number of spectral band and  $m$  is number of material.

The objective function is given as,

$$\min_x \|AX - Y\|_2^2 + \lambda \|x\|_1 + \iota_{R_+}(x)$$

Where,  $\iota_{R_+}(x)$ =indicator function

The objective function can be rewritten after applying the concept of variable splitting as,

$$\min_{U, V_1, V_2, V_3} \frac{1}{2} \|V_1 - Y\|_2^2 + \lambda \|V_2\|_1 + \iota_{R_+}(V_3) \quad (2)$$

Subject to  $V_1=AU \quad V_2 = U \quad V_3=U$

In compact form

$$\min_{U, V} g(V) \quad (3)$$

Subject to  $GU+BV=0$

$$\text{Where, } g(V) = \frac{1}{2} \|V_1 - Y\|_2^2 + \lambda \|V_2\|_1 + \iota_{R_+}(V_3) \quad (4)$$

In which  $V=(V_1, V_2, V_3)$

Given that,  $V_1=AU, V_2 = U, V_3=U$

Using this we can write,

$$\begin{aligned} V_1=AU &\Rightarrow AU - V_1 = 0 \\ V_2 = U &\Rightarrow U - V_2=0 \\ V_3 = U &\Rightarrow U - V_3=0 \end{aligned} \quad (5)$$

Using above equation, we can write in matrix form like,

$$G = \begin{bmatrix} A \\ I \\ I \end{bmatrix} \quad B = \begin{bmatrix} -I & 0 & 0 \\ 0 & -I & 0 \\ 0 & 0 & -I \end{bmatrix}$$

Consider augmented Lagrange multiplier for above equation and it can be written as,

$$\mathcal{L}(U, V, D)=g(U, V) + \frac{\mu}{2} \|GU + BV - D\|_2^2 \quad (6)$$

subject to  $GU + BV=0$

Expansion of above expression is given as,

$$\begin{aligned} \mathcal{L}(U, V_1, V_2, V_3, D_1, D_2, D_3) = & \frac{1}{2} \|V_1 - Y\|_2^2 + \\ & \lambda \|V_2\|_1 + \iota_{R_+}(V_3) + \frac{\mu}{2} \|AU - V_1 - D_1\|_2^2 + \mu \|U - V_2 - \\ & D_2\|_2^2 + \mu \|U - V_3 - D_3\|_2^2 \end{aligned} \quad (7)$$

Pseudocode

When we take optimization with respect to variable U we get:

$$U^{(k+1)} \leftarrow (A^T A + 2I)^{-1} (A^T \varepsilon_1 + \varepsilon_2 + \varepsilon_3) \quad (8)$$

Where,  $\varepsilon_1 = V_1^{(k)} + D_1^{(k)}$

$$\varepsilon_2 = V_2^{(k)} + D_2^{(k)}$$

$$\varepsilon_3 = V_3^{(k)} + D_3^{(k)}$$

For minimization with respect to variable V we get three values of V:

$$V_1^{(k+1)} \leftarrow \frac{1}{1+\mu} [Y + \mu(AU^{(k)} - D_1^{(k)})] \quad (9)$$

$$V_2^{(k+1)} \leftarrow \text{soft}(\varepsilon_2, \frac{\lambda}{\mu}) \quad (10)$$

Where,  $\varepsilon_2 = U^{(k+1)} + D_2^{(k)}$

$$V_3^{(k+1)} \leftarrow \max(U^{(k)} - D_3^{(k)}, 0) \quad (11)$$

Now, we have to Update Lagrange multipliers as:

$$D_1^{(k+1)} \leftarrow D_1^{(k)} - AU^{(k+1)} + V_1^{(k+1)}$$

$$D_2^{(k+1)} \leftarrow D_2^{(k)} - U^{(k+1)} + V_2^{(k+1)} \quad (12)$$

$$D_3^{(k+1)} \leftarrow D_3^{(k)} - U^{(k+1)} + V_3^{(k+1)}$$

After updating Lagrange multiplier, update the value of k by adding 1 and do this iterative process till stopping criterion is satisfied. The CSR problem is solved by using SUnSAL algorithm.

#### IV. SIMULATION RESULT

Performance of SUnSAL algorithm has been tested with the help of synthetically generated Data Cubes (DC). For simulation, subset of original USGS spectral library is used, which contains 498 spectral signatures and denoted with A. Each spectral signature has 224 bands, which is denoted by L. Three data cubes, of size 100 X 100, have been generated using fraction abundance map generated by HYDRA toolbox and randomly selecting spectral signatures from A. For the DC #1 spectral signature number [135, 394, 409] and fractional abundance map as shown in figure are used. Similarly, DC # 2 and DC # 3 are generated using spectral signature number [21 135 176 394 487] and [21 31 129 135 176 377 394 409 487] respectively. Fractional abundance map for DC # 2 and DC #

3 are shown in figure. Signal to Reconstruction Error (SRE) is used as a performance evaluation parameter as,

$$SRE=20 \log_{10} \frac{E[\|x\|_2^2]}{E[\|x-\hat{x}\|_2^2]}$$

Where, x was the estimated fractional abundance vector by the unmixing algorithms. The smaller RMSE meant  $\hat{x}$  (the estimated fractional abundance) was closer to x (the real fractional abundance), which indicate better unmixing performance. SRE gave more information regarding the power of the error in relation with the power of the signal. The Vales of SRE is opposite to RMSE. For the better unmixing performance SRE should be higher.

The synthetically generated data cubes are corrupted with different noise level like 30dB, 40dB, 50dB and 60dB. In this simulation we have measured the value of SRE after 250 iterations for different values of parameter  $\lambda$ .

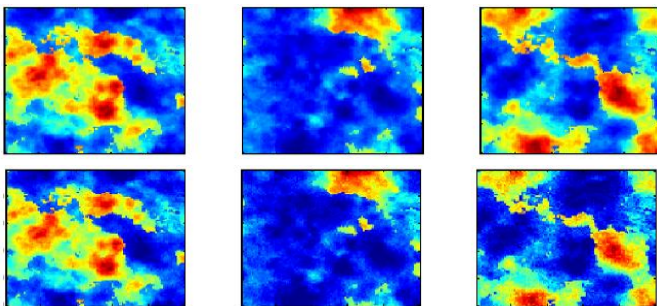


Figure 3. First row shows the abundance map of true endmembers. Second row show the abundance map for estimated endmember.

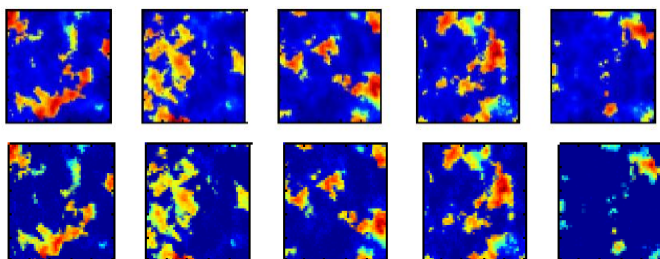


Figure 4. First row shows the abundance map of true endmembers. Second row show the abundance map for estimated endmember.

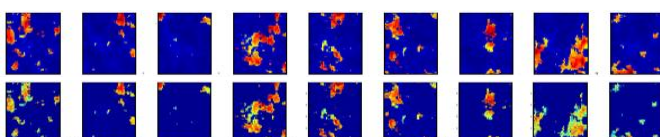


Figure 5. First row shows the abundance map of true endmembers. Second row show the abundance map for estimated endmember.

TABLE I

Results for signal to reconstruction error for image size 64 x 64 and different endmembers.

Endmember	3	5	7	9
SRE (64*64)	15.821	16.553	17.255	12.975

TABLE III

Results for signal to reconstruction error for image size 100 x 100 and different endmember.

Endmber	3	4	5	6	10	15	17	20
SRE	16.546	11.824	11.623	12.244	15.991	15.959	12.906	12.500

This section discusses the simulation results of Signal to Reconstruction Error(SRE) for different values of lambda and different values of signal to noise ratio(SNR) for three, five and seven endmembers respectively for 100 x 100 image size.

TABLE IVVI

Results of signal to reconstruction error and signal to noise ratio for image size 100 x 100 (p=3)

Lambda	0.0005	0.0001	0.001	0.01
SNR(dB)	SRE	SRE	SRE	SRE
30	10.110	8.369	8.421	8.406
40	13.404	13.400	13.438	11.084
50	17.109	17.045	17.200	11.702
60	19.616	19.178	19.412	11.777

TABLE VIV

Results of signal to reconstruction error and signal to noise ratio for image size 100 x 100 (p=5)

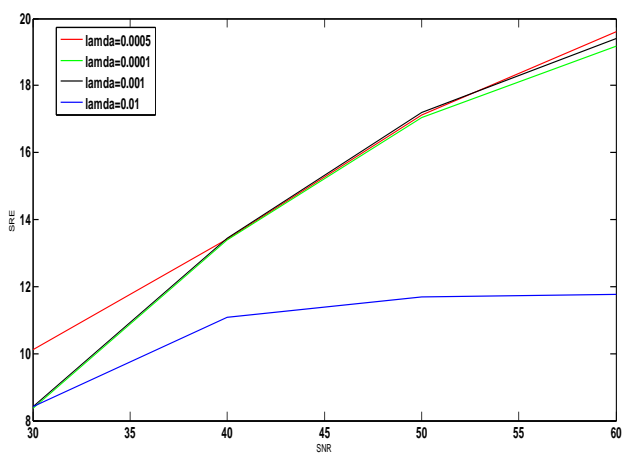
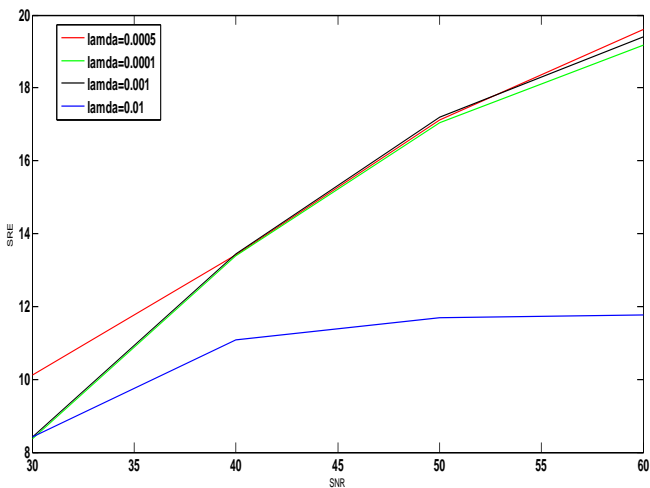
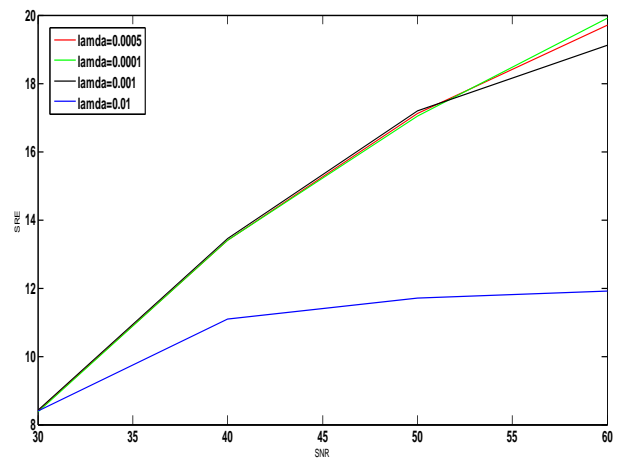
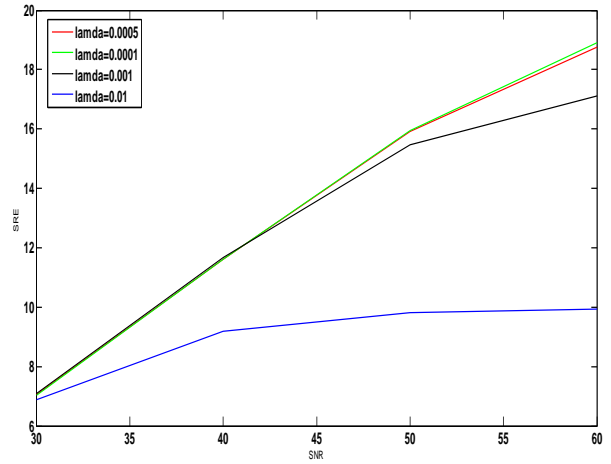
Lambda	0.0005	0.0001	0.001	0.01
SNR(dB)	SRE	SRE	SRE	SRE
30	7.061	7.046	7.094	6.872
40	11.623	11.608	11.664	9.173
50	15.903	15.961	15.453	9.815
60	18.760	18.910	17.113	9.925

TABLE V

Results of signal to reconstruction error and signal to noise ratio for image size 100 x 100 (p=7)

Lambda	0.000	0.000	0.001	0.01
SNR(dB)	SRE	SRE	SRE	SRE
30	8.385	8.369	8.421	8.406
40	13.40	13.40	13.43	11.08
50	17.10	17.04	17.20	11.70
60	19.70	19.90	19.11	11.90

The below figures show the graphical representation of SRE to SNR for 100\*100 image size for three, five and seven endmembers.



### V. CONCLUSIONS

Linear spectral unmixing is emerging topic for the researcher in the field of remote sensing. HU is inverse ill-posed problem. HU is challenging task due to large data size, observation noise, model inaccuracy, different environment conditions and endmember variability. HU is the process to collect number of endmembers, their spectral signature and their abundance map. From the three approaches, sparse regression based approach is selected for HU.

For sparse unmixing SUnSAL algorithm is selected. And it is implemented using USGS spectral library in MATLAB. The contribution of different materials are viewed based on synthetic image and also the implementation is done using SUnSAL algorithm. Plot the SRE (dB) values for different values of white noise, using spectral libraries. SRE is increases with increase in SNR values. Also Plot the SRE (dB) and p values (number of endmembers), which is obtained using spectral library. The obtained synthetic image found to be efficient and effective. Also estimation of abundance matrix is done by using SUnSAL algorithm.

---

REFERENCES

- [1] José M. Bioucas-Dias, Antonio Plaza, Nicolas Dobigeon, Mario Parente, QianDu, Paul Gader and Jocelyn Chanussot, "An overview on hyperspectral unmixing: Geometrical, statistical, and sparse regression based approaches", *IEEE journal of selected topics in applied earth observations and remote sensing*, vol. 5 (no. 2), pp.1135-1138, April 2012.
- [2] J. Liu and J. Zhang, "Spectral Unmixing via Compressive Sensing," in *IEEE Transactions on Geoscience and Remote Sensing*, vol. 52, no. 11, pp. 7099-7110, Nov. 2014.
- [3] M. D. Iordache, J. M. Bioucas-Dias and A. Plaza, "Collaborative Sparse Regression for Hyperspectral Unmixing," in *IEEE Transactions on Geoscience and Remote Sensing*, vol. 52, no. 1, pp. 341-354, Jan. 2014.
- [4] Iordache, M.D.; Bioucas-Dias, J.M.; Plaza, A., "Sparse Unmixing of Hyperspectral Data," *Geoscience and Remote Sensing, IEEE Transactions on*, vol.49, no.6, pp.2014-2039, June 2011.
- [5] MJ. M. Bioucas-Dias and M. A. T. Figueiredo, "Alternating direction algorithms for constrained sparse regression: Application to hyperspectral unmixing," *2012 2nd Workshop on Hyperspectral Image and Signal Processing: Evolution in Remote Sensing, Reykjavik*, pp. 1-4, 2012.
- [6] W. Tang, Z. Shi, Y. Wu and C. Zhang, "Sparse Unmixing of Hyperspectral Data Using Spectral A Priori Information," in *IEEE Transactions on Geoscience and Remote Sensing*, vol. 53, no. 2, pp. 770-783, Feb. 2015.
- [7] Wing-Kin Ma, José M. Bioucas-Dias, Jocelyn Chanussot, and Paul Gader, "Signal and Image Processing in Hyperspectral Remote Sensing", *IEEE signal processing magazine*, pp. 22,23, January 2014.
- [8] USGS Digital Spectral Library: <http://speclab.cr.usgs.gov/spectral-lib.html>
- [9] Ertürk and A. Plaza, "Informative change detection by unmixing for hyperspectral images," in *IEEE Geoscience and Remote Sensing Letters*, vol. 12, no. 6, pp. 1252–1256, June 2015.
- [10] M. D. Iordache, J. M. Bioucas-Dias and A. Plaza, "Sparse Unmixing of Hyperspectral Data," in *IEEE Transactions on Geoscience and Remote Sensing*, vol. 49, no. 6, pp. 2014-2039, June 2011.
- [11] M. D. Iordache, A. Plaza and J. Bioucas-Dias, "Recent developments in sparse hyperspectral unmixing," *2010 IEEE International Geoscience and Remote Sensing Symposium*, Honolulu, HI, 2010, pp. 1281-1284.
- [12] M. D. Iordache, J. Bioucas-Dias and A. Plaza, "Unmixing sparse hyperspectral mixtures," *2009 IEEE International Geoscience and Remote Sensing Symposium*, Cape Town, 2009, pp. IV-85-IV-88.
- [13] <https://www.it.pt/>